Journal of the Geological Society, London, Vol. **164**, 2007, pp. 1133–1144. Printed in Great Britain.

Discrete Plio-Pleistocene phases of tilting and counterclockwise rotation in the southeastern Aegean arc (Rhodos, Greece): early Pliocene formation of the south Aegean left-lateral strike-slip system

DOUWE J. J. VAN HINSBERGEN[1,2], WOUT KRIJGSMAN[1], COR G. LANGEREIS[1], JEAN-JACQUES CORNÉE[3], CHARON E. DUERMEIJER[1] & NICOLE VAN VUGT[1]

[1]*Paleomagnetic Laboratory 'Fort Hoofddijk', Utrecht University, Faculty of Geosciences, Budapestlaan 17, 3584 CD Utrecht, The Netherlands (e-mail: hins@geo.uu.nl)*

[2]*Department of Geology, University of Leicester, University Road, Leicester LE1 7RH, UK*

[3]*UMR CNRS 5125 Paléoenvironnements & Paléobiosphère, Université Claude Bernard Lyon I, 27 Bd. du 11 Novembre 1918, 69622 Villeurbanne Cedex, France*

Abstract: The island of Rhodos represents an uplifted block in the largely submerged southeastern Aegean forearc. It has a complex history of subsidence, uplift and counterclockwise rotation during the Plio-Pleistocene, in response to the interplay between large-scale geodynamic processes. In this paper, we present a new chronostratigraphic framework for the continental Pliocene Apolakkia basin of southwestern Rhodos. We combine these time constraints with recently published chronostratigraphic data from the marine Plio-Pleistocene basins of northeastern Rhodos to reconstruct rotational and vertical motions. Our palaeomagnetic results identify two rotation phases for Rhodos: *c*. 10° ($9 \pm 6°$) counterclockwise (ccw) rotation between 3.8 and 3.6 Ma, and *c*. $17 \pm 6°$ ccw rotation since 0.8 Ma. Between these phases, Rhodos tilted to the SE, drowning the southeastern coast to a depth of 500–600 m between 2.5 and 1.8 Ma, then to the NW, which resulted in the re-emergence of the drowned relief between 1.5 and 1.1 Ma. We relate the rotations of Rhodos to incipient formation of the south Aegean sinistral strike-slip system and the foundering of the Rhodos basin. The previously shown absence of Messinian evaporites in the deep-marine Rhodos basin in combination with the 3.8 Ma onset of ccw rotation of Rhodos constrains the onset of the formation of the south Aegean strike-slip system between 5.3 and 3.8 Ma. The formation of this strike-slip system is probably related to the interplay of oblique collision between the southeastern Aegean region and the northward moving African plate, the westward motion of Anatolia, gravitational spreading of the overthickened Aegean lithosphere and the recently postulated southwestward retreat of the African subducted slab along a subduction-transform edge-propagator fault.

The curvature of the Hellenic arc has increased systematically since Eocene times and has been explained by various scenarios including southward roll-back of subducting African lithosphere and associated back-arc extension, gravitational collapse, or westward extrusion of Anatolia (Dewey & Sengör 1979; Le Pichon & Angelier 1979; Le Pichon 1982; Taymaz *et al*. 1991; Gautier *et al*. 1999; Jolivet 2001). The southeastern Aegean forearc is characterized by left-lateral shear zones, both offshore (Peters & Huson 1985; Mascle *et al*. 1999; Huguen *et al*. 2001; ten Veen & Kleinspehn 2002) and onshore (Duermeijer *et al*. 1998; ten Veen & Postma 1999; ten Veen & Kleinspehn 2002, 2003) (Fig. 1).

Previous palaeomagnetic studies have shown that the region mainly underwent counterclockwise rotation during the Neogene. The Bey Dağları region of southwestern Turkey (Fig. 1) reveals a regionally consistent 30° counterclockwise rotation of sediments of early Miocene age (Kissel & Poisson 1987; Morris & Robertson 1993). Counterclockwise rotations have also been reconstructed from Crete, Kassos and Karpathos (Fig. 1), but a regional inconsistency in amount of rotation of time-equivalent sediments led Duermeijer *et al*. (1998, 2000) and ten Veen & Meijer (1998) to interpret these as local counterclockwise rotations during the Plio-Pleistocene accommodating the left-lateral strike-slip between fault zones trending 070°. Palaeomagnetic data from the Plio-Pleistocene marine successions of Rhodos (Fig. 1) have also indicated counterclockwise rotations, but the available biostratigraphic constraints have hitherto not allowed a precise age estimate (Laj *et al*. 1978, 1982; Løvlie *et al*. 1989; Duermeijer *et al*. 2000).

The island of Rhodos is a key area for assessing the forearc kinematic response to expansion and wrenching of the Aegean–Anatolian domain. Until now, interpretations of the tectonic history of the southeastern Aegean forearc were hampered by the absence of accurate time constraints and stratigraphic control. Here we present a high-resolution stratigraphy for the terrestrial Plio-Pleistocene sediments of the Apolakkia basin of SW Rhodos. These vast continental sequences reflect both tectonic and climatic changes, and deciphering their respective effects on the sedimentation is critical to determining the geodynamic and palaeoenvironmental evolution. Such a study, however, requires an accurate time frame, which is at present largely absent. So far, the Apolakkia sediments have only been roughly dated as early Pliocene (middle–late Ruscinian) based on fossil mammal assemblages (van de Weerd *et al*. 1982). Here, we provide new palaeomagnetic results from Pliocene fluvio-lacustrine successions of the Apolakkia Formation. In contrast to other studies, which focused on tectonics and facies architecture (Meulenkamp *et al*. 1972; ten Veen & Kleinspehn 2002) and glacio-eustatic

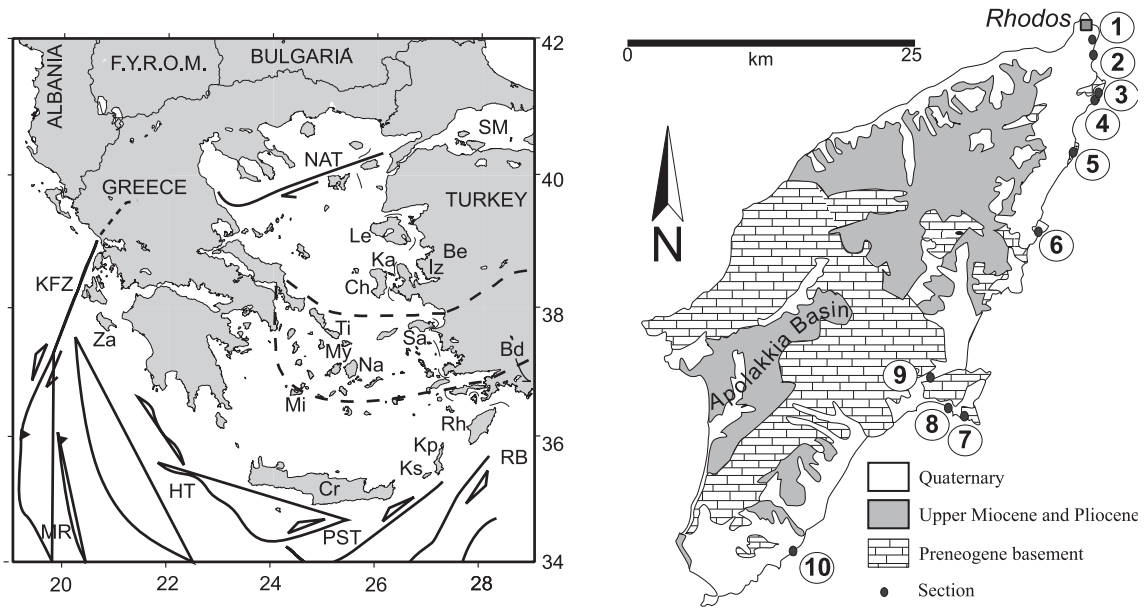

Fig. 1. Geological map of Rhodos, modified after Bornovas & Rontogianni-Tsiabaou (1983). Numbered dots refer to the sections sampled for palaeobathymetry analysis: 1, Sunwing; 2, Eden Roc; 3, Tassos Bay; 4, Faliraki Beach; 5, Ladiko Bay; 6, Kolymbia; 7, Pefki; 8, Pefkos Beach; 9, Agios Ioannis; 10, Plimiri. In inset: Bd, Bey Dağları region; Be, Bergama region; Ch, Chios; Cr, Crete; HT, Hellenic trench; Iz, Izmir region; Le, Lesbos; Mi, Milos; Ka, Karaburun peninsula; KF2, Kephallonian Fault Zone; Kp, Karpathos; Ks, Kassos; MR, Mediterranean Ridge; NAT, North Aegean Thrust; PST, Pliny and Strabo trenches; Sa, Samos; RB, Rhodos basin; Rh, Rhodos; SM, Sea of Marmara; Za, Zakynthos.

sea-level changes (Cornée *et al*. 2006*a*), we examine the potential control of astronomical forcing on the sedimentation.

We use this high-resolution stratigraphic control to accurately date the rotation history of Rhodos through new palaeomagnetic analyses and reinterpretation of previous results. Vertical motion history is based on a palaeobathymetry study of marine Plio-Pleistocene sequences from NE Rhodos. Recently, a new chronology has been presented for these marine sediments (Cornée *et al*. 2006*a*), which allows us to constrain our rotational and vertical motions in a high-resolution time frame. We thus reconstruct the temporal relationships between horizontal (rotational) and vertical motions of Rhodos to add to understanding of the complex interplay between the large-scale geodynamic processes deforming the Aegean region.

Geology of Rhodos

The island of Rhodos is located at the eastern end of the Hellenic arc in the Eastern Mediterranean (Fig. 1). The backbone of the island is formed by a series of stacked and folded tectonic units mainly comprising sediments of Mesozoic and Palaeogene age (Mutti *et al*. 1970). During the Mio-Pliocene, the area was part of a large landmass that was eroded, followed by tectonic extension and formation of a complex series of interlinked grabens and half-grabens. The fill of these basins consists of a Mio-Pliocene non-marine clastic sequence supplied from the east and SE (Meulenkamp *et al*. 1972). The lower non-marine coarse clastic sediments remain poorly dated, and may locally be as old as late Miocene, or possibly middle Miocene (Willmann 1980; Duranti 1997). During the Pliocene, the island was part of a large subsiding fluvial and lacustrine basin, providing ample accommodation space for the large supply of clastic sediments from the east and NE. The area was fragmented by block faulting in the late Pliocene and Pleistocene and freshwater limestones (travertine) were deposited in the south, whereas lagoonal (paralic) and fluvial deposits from this period have been found in other parts of the island. During the Plio-Pleistocene the area became separated from the Turkish mainland and open marine deposition occurred along the present coastline of the island. Here, we present new age constraints for both the non-marine Apolakkia Formation of SW Rhodos and the marine sequences of the northern and eastern coastline of the island.

Fluvio-lacustrine successions of the Apolakkia Formation (SW Rhodos)

The Apolakkia basin in the SW part of Rhodos (Fig. 2) originated as a late Miocene–early Pliocene fault wedge basin in response to syndepositional NE–SW extension with strain patterns similar to the adjacent offshore inner forearc (ten Veen & Kleinspehn 2002). There, the Hellenic 'trenches', which are en enchelon segmented bathymetric troughs, demarcate subparallel left-lateral strike-slip zones within the forearc. During the Plio-Pleistocene, a transtensional phase reoriented the basin and resulted in transtension combining syndepositional WNW–ESE extension and 070° left-lateral shear (ten Veen & Kleinspehn 2002).

The Apolakkia Formation (see Meulenkamp *et al*. 1972) consists of marls, lignitic clays, thin lignites, sands and conglomerates, and unconformably overlies the mainly non-marine coarse clastic deposits of the Istrios Formation (Duranti 1997) (Fig. 2). The abundant freshwater molluscs of the Apolakkia Formation were studied by Willmann (1980) and the rare mammalian remains by van de Weerd *et al*. (1982). In particular, the mammal fauna suggests an early–middle Pliocene age (MN zone 15: Benda *et al*. 1977; van de Weerd *et al*. 1982). The top of the Apolakkia Formation shows a transition toward the freshwater

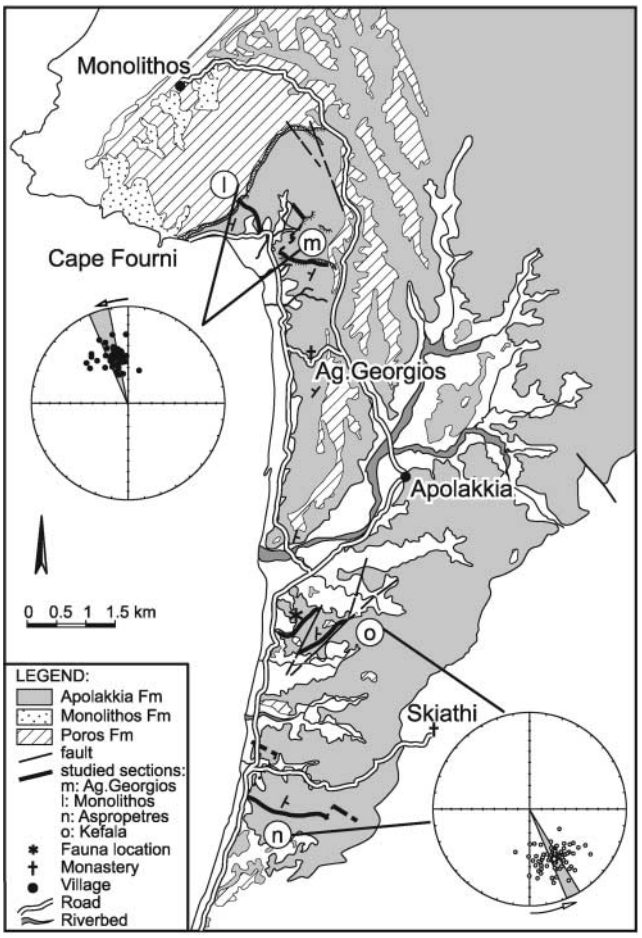

Fig. 2. Geological sketch map of the Apolakkia basin, SW Rhodos. Equal area projections show the characteristic remanent magnetization (ChRM) directions of the four studied sections. ●, downward projections; ○, upward projections. Grey arcs give the α_{95} cones of 95% confidence for the various site means. Arrows indicate sense of observed tectonic rotation.

limestones and travertines of the Monolithos Formation. This latter formation has remained undated prior to the present study.

On a tens-of-metres scale, the Apolakkia Formation shows a cyclic alternation of different lithofacies. To describe the cyclicity, three facies associations are distinguished: delta plain, palustrine and shallow lacustrine (Duranti 1997). The subaerial delta plain association consists of graded sand, silt and calcretes (abundant carbonate concretions in palaeosols). The palustrine association is dominated by dark marl and lignite, with minor intercalations of beige marls, palaeosols and sand sheets. The depositional environment of the palustrine facies was a regularly flooded swamp or vegetated mud flat along the margin of a lake. The shallow lacustrine association consists of an alternation of lacustrine marl, pedogenic carbonate (palaeosols), lignite and sand, deposited on the margin of a large lake with varying water levels, which regularly caused desiccation (Duranti 1997).

In the central part of the Aspropetres section, the sedimentary cycles are *c*. 35 m thick. The cyclic pattern is very regular, suggesting a relationship to astronomically induced changes in the regional climate (van Vugt 2000). The delta plain association generally crops out as a dip slope, followed by dark organic-rich layers of the palustrine facies association. Upwards, the thickness, frequency and darkness of these beds decrease, and the beige marl, silt and sandstone of the shallow lacustrine facies association predominate. This is followed by the next coarse-grained interval of the delta plain association. The sedimentary cyclicity in the Monolithos section does not always show the palustrine association, and the marginal lacustrine association can appear different because of the lacustrine limestone and sandstone beds. Nevertheless, regularly spaced (*c*. 25 m) coarse-grained beds are laterally continuous over the width of the exposure (several hundreds of metres). On the assumption that these cycles are orbitally forced the sedimentation rate in the Monolithos section is inferred to have been slightly lower than that in the Aspropetres section.

Terrestrial to marine successions of northeastern and eastern Rhodos

In northeastern Rhodos, sedimentation started later. Here, a Turolian to Ruscinian (late Miocene to early Pliocene) mammalian fauna was found in a fissure overlain by coarse fluvial conglomerates with westward palaeoflow directions (Maritsa conglomerates: de Bruijn *et al*. 1970; Meulenkamp *et al*. 1972). The deposition of the Maritsa conglomerates was followed by a transgression, ultimately leading to the deposition of open marine clays along the present-day southeastern coast of Rhodos (Meulenkamp *et al*. 1972; Hanken *et al*. 1996). These open marine clays are confined to a small strip along the eastern coast of Rhodos, where they unconformably overlie pre-Neogene basement (e.g. Pefki) or late Pliocene shallow-marine sediments and indicate drowning of a coastal palaeorelief (Meulenkamp *et al*. 1972; Broekman 1974; Moissette & Spjeldnæs 1995; Hanken *et al*. 1996; Kovacs & Spjeldnæs 1999; Titschack *et al*. 2005). Cornée *et al*. (2006*a*, *b*) recently showed that sedimentation continued into the late Pleistocene, to 0.3 Ma, during deposition of a newly defined Ladiko–Tsampika Formation.

We have sampled 10 short sedimentary sections for palaeobathymetry analysis of these marine deposits (Fig. 1). Løvlie *et al*. (1989) published a magnetostratigraphy for the open marine clays of the Kolymbia section (Fig. 1) and correlated it with the Gilbert, Gauss, Matuyama and part of the Bruhnes chrons; that is, *c*. 3.5–0.5 Ma (Lourens *et al*. 2004). However, they did not provide biostratigraphic evidence to confirm a 3 Ma timespan, and later Løvlie & Hanken (2002) noted a strong present-day field overprint in these samples. Duermeijer *et al*. (2000) resampled the section for rotation analysis and their samples were all reversed. Løvlie *et al*. (1989) reported *Hyalinea balthica* in the top of the section although this was not confirmed by Frydas (1994) or Cornée *et al*. (2006*a*). Only the presence of *Globorotalia inflata* throughout the section (Spaak 1983; Cornée *et al*. 2006*a*) indicates an age younger than 2.09 Ma (Lourens *et al*. 2004), and therefore Cornée *et al*. (2006*a*) correlated the Kolymbia (or Cape Vagia) section to the Olduvai subchron (1.942–1.785 Ma: Lourens *et al*. 2004). This interpretation is corroborated by the dating of a volcanic ash layer to 2.06 ± 0.14 Ma in comparable facies to the SW of Kolymbia (Cornée *et al*. 2006*a*). The Pleistocene was further sampled in sections at Sunwing, Eden Roc, Tassos Bay, Faliraki Beach (described by Sørensen (1984)), Pefkos Beach and Plimiri. These sections all contain *Hyalinea balthica* (see also Thomsen *et al*. 2001), indicating an age younger than 1.49 Ma (Lourens *et al*. 1998).

West of Pefki and Pefkos Beach, a small outcrop of calcareous marls is exposed in the turn of the road just NE of the chapel of

Aghios Ioannis. Age markers in these sediments are very rare and show evidence for reworking of early to late Pliocene marine sediments. The age remains unresolved. The top of the stratigraphy is formed by Pleistocene shallow-marine coarse cross-bedded calcarenites (Hansen 1999), belonging to the Tsampika–Ladiko Formation, which is considered to have been deposited between *c*. 1.3 and 0.3 Ma (Cornée *et al*. 2006*a*). It unconformably overlies sections at Eden Roc and Faliraki Beach and conformably progrades over the section at Tassos Bay (Fig. 1). Nine depositional sequences (TS1–TS9) were identified in the Tsampika–Ladiko Formation, consisting mainly of conglomerates, sandstones and monotonous greenish silty clays deposited in retrogradational–progradational paralic sequences interpreted to reflect cyclic sea-level changes related to glacial–interglacial 100 ka cycles (Cornée *et al*. 2006*a*).

Palaeomagnetism: methods and procedure

We have logged and sampled four sections of the Apolakkia Formation that are not disturbed by faults with displacement exceeding a few metres (Fig. 2). In all sections, oriented hand samples were taken from holes dug deeply below the weathered crust to avoid overprint of the magnetization because of weathering. In the laboratory, 2.5 cm diameter cores were drilled from these hand samples, and cores were cut into 2.2 cm long specimens.

Thermomagnetic runs in air were carried out on selected samples, to determine unblocking temperatures of minerals carrying the remanence, and to monitor possible changes in magnetomineralogy by heating. In the thermomagnetic curves of the fresh clay samples, there is a relatively small but significant increase starting at 390 °C, typical of the alteration of pyrite into magnetite. However, the contribution is not visible in the thermal demagnetization diagrams (Fig. 3a), because it is small compared with the magnetite content of the samples and does not lead to disturbance of magnetizations at higher temperatures. The highest unblocking temperatures are close to, or slightly above, 580 °C, identifying (partly maghemized) magnetite as the carrier (Fig. 3a and b). The other lithologies have no such pyrite peak, and maximum unblocking temperatures are close to 580 °C (magnetite) for fresh silt, and slightly higher, up to 610 °C (maghemized magnetite) for coarser material and weathered rock (Fig. 3d). We thus conclude that the fresh clay and silt samples contain mainly magnetite, a stable carrier for natural remanent magnetization (NRM). In fresh clays, it is likely that magnetic iron sulphides (such as greigite or pyrrhotite) are additionally present, considering the higher fields required to saturate the isothermal remanent magnetization (IRM) (>400 mT, Fig. 3c). Weathering has probably caused (partial) oxidation of the magnetic iron sulphides, especially in coarser-grained samples, as is evident from the normal overprint in these samples and from the faster decay of the intensity at low temperatures, compared with the Fe-sulphide-bearing samples (Fig. 3d).

NRM was measured on a 2G-SQUID cryogenic magnetometer and samples were thermally demagnetized in steps of 50 °C. The NRM intensity varies between 0.1 and 70 mA m^{-1}, with an average of 3 mA m^{-1} in the Aspropetres and Monolithos sections and 17 mA m^{-1} in the generally coarser-grained Agios Georgios section. Fresh clay samples show a first decay of the NRM around 350 °C, followed by a second decay to *c*. 580 °C, again suggesting that a magnetic Fe sulphide (such as greigite) also carries a remanence component. The demagnetization diagrams of unweathered silty material show generally one component, which is fully demagnetized after heating to 580–620 °C (Fig. 3). The samples from weathered rocks have an additional low-temperature component that is completely removed by 250 °C (Fig. 3), which we interpret as a present-day field overprint caused by weathering.

Magnetostratigraphic dating of the Apolakkia basin fill

The Kefala and Aspropetres sections record only reversed polarities, whereas the Agios Georgios and Monolithos sections show both normal and reversed polarities (Fig. 4). The stratigraphical interval between the Agios Georgios and Monolithos sections is estimated (using a topographical map and average bedding orientation) to be 200–350 m. van de Weerd *et al*. (1982) assigned the Kefala section to mammal zone MN 15, which is dated between 4.2 and 3.6 Ma (Agustí 2001). The long reversed interval from the Aspropetres section can therefore only represent the top of the Gilbert Chron (Fig. 4). Assuming constant sedimentation rates for each interval shown in Figure 4 we estimate the age of the top of the Aspropetres section at 3.8 Ma. The normal-polarity intervals in the stratigraphically younger sections thus probably represent parts of the Gauss Chron. The correlation of our newly obtained magnetostratigraphy to the polarity time scale of Lourens *et al*. (2004) is shown in Figure 4. Other possible correlations have been investigated, but result in unrealistic changes in sedimentation rate and are considered as less likely (see van Vugt (2000) for discussion).

Astronomical forcing of sedimentary cyclicity in the Apolakkia Formation

To test for astronomical forcing of sedimentary cyclicity in the Apolakkia Formation, our magnetostratigraphic results can be used to investigate whether the average periodicity of the sedimentary cycles matches one of the known astronomical frequencies. In Aspropetres, the average thickness of the observed lithological cycles is *c*. 35 m. With a minimum sedimentation rate of 1.35 m ka^{-1} this predicts a maximum average duration of 27 ka per cycle. For Monolithos, the average duration is between 24 and 33 ka per cycle, depending on the exact number of cycles (3.5 or 3) in the Kaena interval (Fig. 4). The average period of the precession cycle (22 ka) is thus comparable with the results from both sections and suggests that the

Fig. 3. Typical demagnetization diagrams of a fresh (**a**) and a weathered (**b**) sample. ● (○), horizontal (vertical) projection of the magnetic direction. (**c**) Relative magnetization v. applied field in an IRM acquisition experiment. Three groups can be distinguished: △, fresh samples; ●, weathered samples; ○, example of a fresh clay sample that does not saturate below 800 mT. (**d**) IRM intensity decrease during stepwise heating: fresh clay samples show a linear decrease (●); weathered samples and sand have a concave pattern (○); fresh silt shows intermediate behaviour (□). (**e**) and (**f**) Curie-balance experiment. During heating, the fresh clay sample has a peak above 400 °C (**e**), whereas the coarser-grained and weathered samples show no such increase in magnetization (**f**). (**g**) Plots of elongation and inclination v. flattening factor (f), as well as elongation v. inclination (thick line) for the TK03.GAD model (Tauxe & Kent 2004), for the data of the combined Ag. Georgios & Monolithos and Kefala & Aspropetres sections, for different values of the flattening factor (f = 0.3 to 1.0). The barbs on the thick line indicate the direction of elongation of the directional distributions, with horizontal being east–west and vertical being north–south. Also shown are results from 20 bootstrapped datasets (thin dashed lines). The crossing points represent the inclination–elongation pair most consistent with the TK03.GAD model (solid thin line). The histograms represent the crossing points from 5000 bootstrapped datasets and show the most frequent inclination (vertical thick line) with 95% bounds (dashed thick lines), compared with the original inclination (vertical thin line) and the crossing points of the original distribution (thin dashed line). The corrected inclination is in good agreement with the geocentric axial dipole (GAD) inclination (55°) for the present latitude of Rhodos, particularly in the case of the combined result of the Kefala and Aspropetres sections.

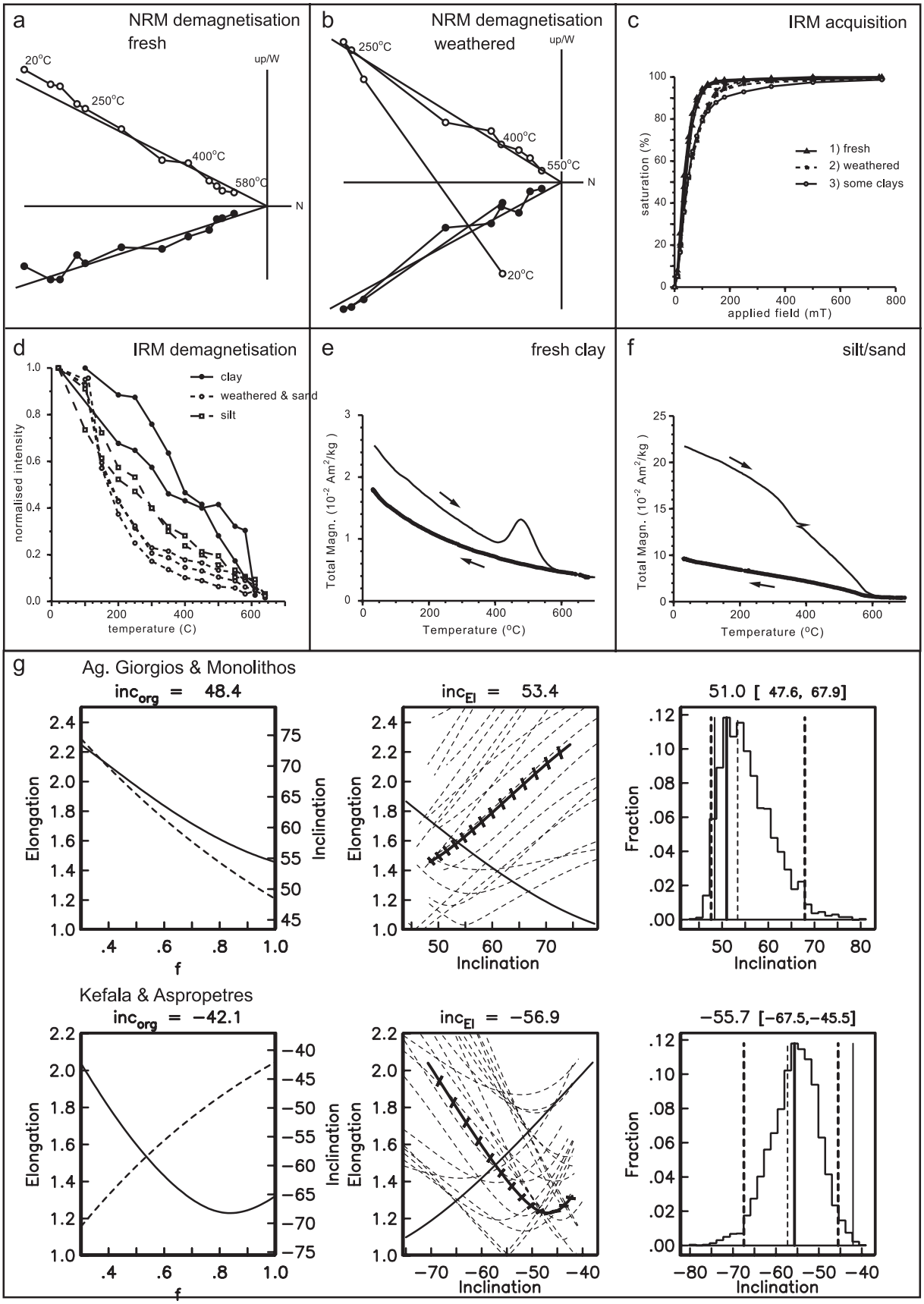
a
NRM demagnetisation
fresh
20°C
250°C
400°C
580°C
up/W
N
b
NRM demagnetisation
weathered
250°C
400°C
550°C
20°C
up/W
N
c
IRM acquisition
saturation (%)
applied field (mT)
1) fresh
2) weathered
3) some clays
d
IRM demagnetisation
clay
weathered & sand
silt
normalised intensity
temperature (C)
e
fresh clay
Total Magn. (10-2 Am2/kg)
Temperature (°C)
f
silt/sand
Total Magn. (10-2 Am2/kg)
Temperature (°C)
g
Ag. Giorgios & Monolithos
inc org = 48.4
Elongation
Inclination
f
inc El = 53.4
Elongation
Inclination
51.0 [47.6, 67.9]
Fraction
Inclination
Kefala & Aspropetres
inc org = −42.1
Elongation
Inclination
f
inc El = −56.9
Inclination
Elongation
−55.7 [−67.5,−45.5]
Fraction
Inclination

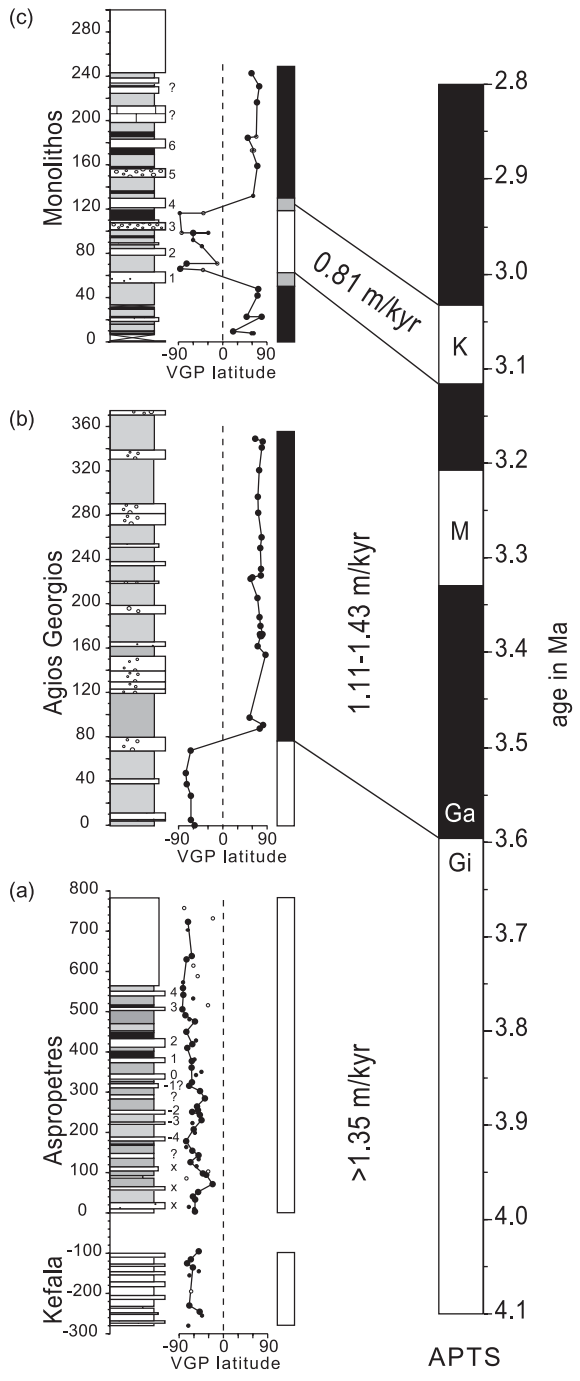

Fig. 4. Schematic representation of the Aspropetres (**a**), Agios Georgios (**b**) and Monolithos (**c**) sections. ●, reliable palaeomagnetic directions; ○, less reliable directions; white indicates reversed polarity; black indicates normal polarity. The lithological column shows coarse-grained beds from the delta plain facies association (dip slopes in Aspropetres) as protruding. Dotted areas indicate sand or conglomeratic sand; areas with circles indicate coarse conglomerate. Light shading indicates marginal lacustrine facies association; dark shading indicates palustrine facies association. The polarity patterns of the studied sections on a single scale is correlated to the polarity time scale. Inferred sedimentation rates are indicated for each interval. APTS, Astronomically tuned polarity time scale.

lithological cycles are indeed astronomically forced, with precession as the dominant parameter. The change in lithology from the Apolakkia Formation to the travertines of the Monolithos Formation can now be estimated to have lasted 40–60 ka (2–3 cycles). This change from detrital clastic sedimentation to chemical carbonate precipitation implies that the supply of clastic material temporarily stopped, although some pebbly sandstones occur between the two travertine beds and above the uppermost travertine (not shown in the log).

Vertical axis rotations of Rhodos

The palaeomagnetic results from samples of the Apolakkia Formation can also be used for rotational studies with the direct benefit of an accurate age control. For this purpose, we select the thermal demagnetization diagrams of the highest quality, showing a linear decay towards the origin. Least-square fitting of lines (Kirschvink 1980) through selected data points was used to determine the directions of the characteristic remanent magnetization (ChRM). The magnetization vectors were averaged using Fisher statistics (Fisher 1953) to calculate mean directions per section. The ChRM results of the four sections of the Apolakkia basin all reveal counterclockwise (ccw) rotations, with mean values of $17 \pm 6°$ ccw for the younger Monolithos and Ag. Georgios sections, and $26 \pm 5°$ ccw for the older Kefala and Aspropetres sections (Table 1). We have applied the reversal test of McFadden & McElhinny (1990) to the Monolithos and Ag. Georgios sections and both yield a positive test (class C; Fig. 5). In addition, we note that both younger sections have a common true mean direction (ctmd, according to the criteria of McFadden & Jones (1981) and McFadden (1990). We performed the same test on the older Kefala and Aspropetres sections, which also share a ctmd. Hence, we can combine all results of the two localities.

It further appears that, in addition to a clearly different amount of ccw rotation, the mean inclinations of the two localities (48.4° and 42.1°, respectively; Table 1) are significantly lower than the expected geocentric axial dipole (GAD) field inclination ($I_{GAD} = 55°$ for the present latitude of Rhodos), particularly for the older two sections. Clearly, the lower inclination cannot be caused by northward movement of Rhodos since the Pliocene. We have therefore applied the inclination error correction according to the field model TK03.GAD (Tauxe & Kent 2004; Fig. 3), as previously applied successfully to Neogene samples from Crete (Krijgsman & Tauxe 2004). In the case of the Kefala–Aspropetres locality, the correction yields a significantly improved inclination (55.7°), indistinguishable from I_{GAD}, suggesting that the NRM was acquired at an early stage and before compaction. In the Monolithos–Ag. Georgios locality, the correction only slightly improves the inclination (51°), and both the original and corrected inclinations are within the error limit of the bootstrapped data. This may be caused by either of the following: (1) these younger sediments more faithfully record the field (and have less compaction); (2) the NRM was acquired at a later stage, during or after compaction, implying a delayed NRM acquisition.

Our results are in good agreement with earlier rotational data for 13 Plio-Pleistocene sites on Rhodos (Fig, 5; Table 1), which indicate only counterclockwise rotations and an average ccw rotation of 18° (Duermeijer *et al*. 2000). Laj *et al*. (1978) reported a 23° ccw late Neogene rotation for Rhodos, although they later concluded that there was no conclusive evidence for any rotation (Laj *et al*. 1982). These studies all lacked absolute

Table 1. *Results from NRM analysis from the different sections and sites on Rhodos*

Site or section	Code	*n*	*D*	*I*	*k*	α95	α95*	Rotation	Age
Tsambika	a	7	163.6	−29.8	37.3	10			Pleistocene
Ladiko	b	9	335.1	29.6	44.8	7.8			Pleistocene
Pefki Beach	c	12	173.0	−49.8	42.6	6.7			Late Plio-Pleistocene
Vagies	d	4	351.2	18.8	26.1	18.3			Late Pliocene
Kallithea	e	4	157.1	−36.9	36.7	15.4			Late Pliocene
Falliraki	f	8	348.7	48.6	70.0	6.7			Late Pliocene
Falliraki Beach	g	11	337.7	63.0	56.8	6.1			Late Pliocene
Kolimbia	h	17	165.8	−42.2	18.2	8.6			Late Pliocene
Pylonas	i	6	160.2	−42.0	21.4	14.8			Late Pliocene
Skaloniti	j	5	168.9	−51.0	324.2	4.3			Late Pliocene
Ancient Kameiros	k	19	352.8	45.8	9.4	11.6			Pliocene
All	a–j, o–p	102	344.9	41.8	38.0	7.5	13.1	15° ccw	Late Plio-Pleistocene
Monolithos (N)		9	339.3	40.5	36.8	8.6			
Monolithos (R)		5	170.3	−52.7	24.0	15.9			
Monolithos	l	14	342.7	44.9	27.0	7.8			3.2–2.9 Ma
Ag. Georgios (N)		23	343.2	50.2	65.9	3.8			
Ag. Georgios (R)		5	160.9	−49.4	41.4	12.0			
Ag. Georgios	m	28	342.8	50.1	62.4	3.5			3.6–3.4 Ma
Both	m + n	42	342.7	48.4	43.2	3.4	6.1	17° ccw	3.6–2.9 Ma
Aspropetres	n	48	153.4	−44.0	36.0	3.5			4.2–3.6 Ma
Kefala	o	27	154.3	−38.5	30.2	5.1			4.2–3.6 Ma
Both	k + l	75	153.7	−42.1	33.0	2.9	5.1	26° ccw	4.2–3.6 Ma

Sites are corrected for bedding tilt. Localities k–n are new, others are taken from Duermeijer *et al*. (2000). Code refers to locations in Figure 5; *n*, number of specimens; *D*, declination; *I*, inclination; *k*, precision parameter of Fisher (1953); α95, 95% cone of confidence; α95*, 95% confidence limits of the declination, calculated as α95/cos *I*, with the expected inclination for Rhodos in the Pliocene of 55°.

age control of the rotational phase(s) on Rhodos because precise age estimates were not available for most of the studied sites.

Our new magnetostratigraphic results combined with additional biochronological and recently published bio- and magnetostratigraphic data on the Plio-Pleistocene (Duermeijer *et al*. 2000; Cornée *et al*. 2006*a*) provide improved age control for the rotation history of Rhodos. The Kefala and Aspropetres sections are the oldest well-dated sections and cover the *c*. 4.2–3.8 Ma interval (Fig. 4). These sections underwent 26 ± 5° ccw rotation (Fig. 5, Table 1). The younger sections of Ag. Georgios (*c*. 3.6–3.4 Ma) and Monolithos (*c*. 3.2–2.9 Ma) underwent 17 ± 6° ccw rotation. We also combined the most reliable reversed ChRM directions obtained by Cornée *et al*. (2006*a*) from the Ladiko–Tsampika Formation with the earlier results from the reversed Tsampika site of Duermeijer *et al*. (2000) to obtain a mean *D*/*I* direction of 163°/−30° (Table 1). The youngest rotated site is now attributed to the Ladiko–Tsampika Formation and has a magnetostratigraphically calibrated age of 1.1–0.8 Ma (Fig. 5, Table 1). Consequently, we conclude that the vertical axis rotation on Rhodos can be subdivided into two phases: 9 ± 6° ccw rotation between 3.8 and 3.6 Ma, and 17 ± 6° ccw rotation since 0.8 Ma (Fig. 5).

Palaeobathymetry and vertical motions

To estimate the depositional depth of the marine sediments of northeastern Rhodos, we use the general relationship between the fraction of planktonic Foraminifera with respect to the total foraminiferal population (%P) and depth of van der Zwaan *et al*. (1990), following sample selection and counting procedures of van Hinsbergen *et al*. (2005*a*). Because the %P also varies with oxygenation, all samples with a fraction of benthic Foraminifera indicating disoxic conditions (stress markers) with respect to the total benthic population exceeding 60% were discarded. Some samples contained high fractions of quartz and rock fragments at deep-marine levels, indicating downslope transport. These samples were discarded, or considered to give a minimum depth value. The depth estimates and their standard deviation (Table 2) were checked by means of presence or absence of benthic depth markers (for details, see van Hinsbergen *et al*. (2005*a*)). These results, especially in the area around Pigadia, are more reliable than the calculated values, which are affected by the influence of downslope sediment transport and/or winnowing. Our palaeobathymetry estimate for Kolymbia of 500–600 m is comparable with the estimate of Moissette & Spjeldnæs (1995), which was based on bryozoans.

Bathymetry is influenced by sedimentary infill, eustatic sea-level changes and tectonics. Our age control does not allow correction for eustatic sea-level changes of tens of metres. The amount of sediment that accumulated in the Pliocene marine setting of Rhodos is negligible compared with the water depths, and sedimentary infilling cannot explain significant shallowing (Fig. 1, Table 2).

Following early Pliocene sedimentation in the Apolakkia basin during NE–SW extension, NW–SE extension changed the palaeoflow direction from westward to east to southeastward in the late Pliocene (Meulenkamp *et al*. 1972). Moreover, the northern and eastern part of the island became submerged (Meulenkamp *et al*. 1972). The palaeobathymetry analysis indicates two distinct phases of vertical motion: the first phase includes tilting to the SE and drowning of the southeastern coast without submergence of the rest of the island. The bulk of this phase occurred prior to, or within, the Olduvai subchron (1.942–1.785 Ma: Lourens *et al*. 2004), because of the deep-marine conditions reconstructed from the Kolymbia section (Fig. 1; Table 2). The onset of subsidence cannot be established with high precision, but probably began around 2.5 Ma, based on the stratigraphic chart of Cornée *et al*. (2006*a*). Deep-marine conditions prevailed until after the first occurrence of *Hyalinea balthica*, around 1.5 Ma, which is found in the rest of our deep-marine sections, although it is not impossible that uplift and re-emergence had already started before that time. The obtained

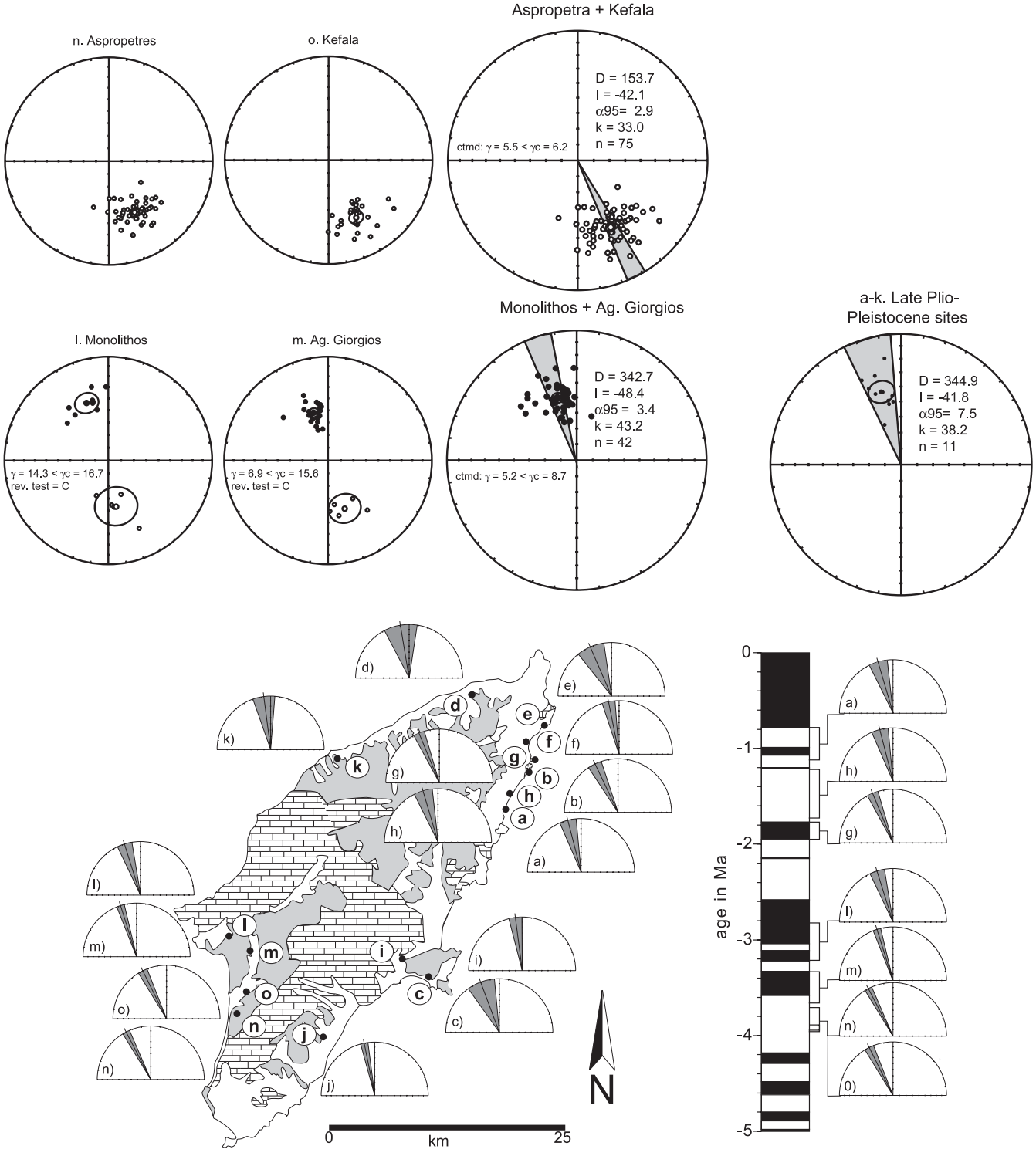

Fig. 5. Equal area plots of the late Pliocene–Pleistocene site averages (a–k in Table 1) showing on average a 15° counterclockwise (ccw) rotation. The ChRM directions of the Ag. Georgios and Monolithos sections show both normal and reversed directions; both sections show a positive reversal test (McFadden & McElhinny 1990) classified as C, and the two section means also show a common true mean direction (ctmd) according to the statistical approach of McFadden (1990). The ChRM directions of the Kefala and Aspropetres sections show only reversed directions; the two section means have a ctmd. The angle between the means (γ) is in all cases smaller than the critical angle (γ_c), indicating a ctmd, which in the case of antipodal directional distributions implies a positive reversal test.

Table 2. *Calculated and estimated palaeobathymetry values for all sites and sections*

Locality	Code	Sample number	*n*	Depth (m)	SD (m)	Taxonomic estimate	Age range
Sunwing	1	12792-95	4	69	25	100–300	Pleistocene
Eden Roc	2	12796-804	5	342	170	200–500	Pleistocene
Tassos Bay	3	12763-65	2	57	20	0–50	Pleistocene
Faliraki Beach	4	12750-62	9	445	209	300–500	Pleistocene
Ladiko Bay	5	12937-48	7	51	25	0–50	Late Plio-Pleistocene
Kolymbia	6	3164-3204	33	283	210	500–600	Pleistocene
Pefki	7	3205-29; 12768-73	28	638	265	300–500	Pleistocene
Pefkos Beach	8	12774-88	11	510	162	300–500	Pleistocene
Aghios Ioannis	9	12766-67				Unreliable	Reworked
Plimiri	10	101-113; 3230-33	13	167	69	200–300	Pleistocene

Sample number refers to samples held in the collection of the Faculty of Geosciences, University of Utrecht. Code refers to numbers in Figure 1. *n*, number of samples averaged; SD, standard deviation.

depth values appear to increase along the coast from NE to SW from 100–300 to 500–600 m, but the chronostratigraphic control is not precise enough to determine whether this trend represents a palaeoslope or different stages in the vertical motion history. The shallow-marine calcarenites and terrestrial sediments of the Ladiko–Tsampika Formation (see Cornée *et al*. 2006*a*) indicate that by 1.1 Ma Rhodos must have been backtilted to the NW for the southeastern coast to re-emerge. The northwestward tilting of Rhodos is still active at present, as concluded by Hanken *et al*. (1996) and Kontogianni *et al*. (2002), based on raised notches and raised beaches of late Pleistocene and Holocene age.

Discussion

The palaeomagnetic and palaeobathymetric analyses show that the late Miocene–early Pliocene phase of extension that opened the Apolakkia basin (ten Veen & Kleinspehn 2002) was followed by four well-dated tectonic phases in the Plio-Pleistocene geological history of Rhodos. Between 3.8 and 3.6 Ma, Rhodos underwent 9° ccw rotation. This was followed between *c*. 2.5 and *c*. 1.8 Ma by southeastward tilting and up to 500–600 m of subsidence of the southeastern coast, leaving the rest of the island above sea level. Between *c*. 1.5 and 1.1 Ma, Rhodos tilted to the NW and the southeastern coast re-emerged above sea level. A tectonic phase of 17° ccw rotation must subsequently have occurred some time after 0.8 Ma. From these results it may be concluded that rotation and tilting occur separately and probably reflect different tectonic processes.

The northwestward tilting of Rhodos between 1.5 and 1.1 Ma that follows from our vertical motion study has already been suggested by Kontogianni *et al*. (2002) to be related to an offshore thrust fault imaged by Woodside *et al*. (2000). The southeastward tilting of Rhodos between 2.5 and 1.8 Ma cannot be correlated in a straightforward way with a single fault motion. We may speculate that the present-day thrust inverted a normal fault along which Rhodos became submerged in the early Pleistocene. Alternatively, or additionally, the drowning is likely to be related to the foundering of the Rhodos basin, although the structural control for the subsidence remains unconstrained.

The emergence of the subhorizontal marine Pleistocene of southeastern Rhodos involved *c*. 500–600 m of uplift. Hanken *et al*. (1996) constructed the axis of tilting, running approximately parallel to the western coast, at a distance of tens of kilometres from the eastern coast. To illustrate that the subhorizontal orientation of the sediments at present does not challenge the tilting scenario of Hanken *et al*. (1996), straightforward trigonometric calculation shows that *c*. 1–2° of northwestward tilting would be sufficient to explain the reconstructed uplift. The vertical motions we have reconstructed have rates of the order of 100 cm ka^{-1} or more for the southeastern coast of Rhodos, during both uplift and subsidence. The amount of uplift of the southeastern coast of Rhodos is confirmed by marine terraces at elevations of more then 500 m (Cornée *et al*. 2006*a*). Cornée *et al*. (2006*a*) suggested that subsidence rates were even higher, based on the assumption that the shallow-marine Kolymbia limestone was deposited within the Olduvai subchron, and that subsidence from 0 to 500 m occurred within the Olduvai (i.e. within *c*. 200 ka), leading to a subsidence rate of *c*. 250 cm ka^{-1}. Although exceptionally high, these rates are comparable with vertical motion results from other regions of the Aegean forearc (van Hinsbergen *et al*. 2004, 2006; van Hinsbergen & Meulenkamp 2006), in Italy (van der Meulen *et al*. 1999, 2000) and southern Spain (Krijgsman *et al*. 2006). Earlier palaeomagnetic results obtained from Zakynthos in the western Aegean region indicated clockwise rotations of *c*. 22° within the last 770 ka and are probably related to dextral wrenching along the Kefallonia Fault Zone offshore northwestern Greece (Duermeijer *et al*. 1999; van Hinsbergen *et al*. 2005*b*). The Zakynthos data are comparable in size, timing and possibly also in rate with the results from Rhodos. These analogues indicate that magnitudes and timings of vertical and rotational motions of Rhodos are typical of their geological context.

To evaluate the regional tectonic importance of these vertical and rotational motions, we first compare the rotation history of Rhodos (9° ccw rotation between 3.8 and 3.6 Ma, and 17° ccw rotation after 0.8 Ma) with the rotation information from the surrounding region. This is comparable with the rotation value we obtained for Rhodos since 3.8 Ma (Table 1). North of Rhodos, no significant rotation ($6 \pm 4°$ ccw) since the middle Miocene was reported from Samos (Sen & Valet 1986), $25 \pm 12°$ ccw rotation from the middle Miocene of Chios (Kondopoulou *et al*. 1993), no significant clockwise rotation since the middle Miocene on Lesbos ($4 \pm 7°$ cw by Beck *et al*. (2001), $12 \pm 15°$ cw by Kondopoulou (1982) and $6 \pm 7°$ cw by Kissel *et al*. (1987, 1989)), highly varying rotations in western Turkey, adjacent to Chios, since the Eocene (49° cw rotation on the Karaburun peninsula, but near Izmir 33° ccw and near Bergama 22° cw (Kissel *et al*. 1987, 1989)) (see Fig. 1 for locations). These data do not show any regional consistency and are as a consequence, at least in part, of local origin. Our results from Rhodos do not put any constraints on the rotation history further north. West of Rhodos, Duermeijer *et al*. (1998) reported highly variable but

consistently counterclockwise rotations since the late Miocene of Crete. They concluded that this pattern resulted from the left-lateral strike-slip deformation associated with southwestward wrenching along the Pliny and Strabo trenches. Alternatively, the Bey Dağları region in adjacent southwestern Turkey has been constrained as a regionally consistent 30° ccw rotation since the earliest Miocene (Kissel & Poisson 1987; Morris & Robertson 1993). The rotation of Rhodos can therefore be related to either rotation mechanism. If Rhodos had been part of the Bey Dağları block, the rotation of Bey Dağları would be late Pliocene and Pleistocene in age. The rotating domain would be *c*. 400 km long, and its 30° ccw rotation would require accommodation through approximately north–south extension to its north, where no consistent counterclockwise rotation was encountered (see above). Simple trigonometry shows that, at the longitude of Rhodos, 30° ccw rotation of a 400 km wide block requires *c*. 200 km of north–south extension since 3.8 Ma. This is far from any reasonable estimate of Aegean extension, which amounts to *c*. 300 km since the Oligocene (Jolivet 2001), largely accommodated in core complexes of early to middle Miocene age. The rotation of the Bey Dağları region in southwestern Turkey is therefore probably much older than the rotation of Rhodos, and could have been accommodated by the early to late Miocene exhumation of the Menderes core complex through north–south extension in western Turkey.

Rhodos is situated within a framework of left-lateral strike-slip faults that form the Pliny and Strabo trenches (Peters & Huson 1985; Mascle *et al*. 1986; ten Veen & Kleinspehn 2002), which are still active today and accommodate *c*. 4 cm a^{-1} of southwestward motion of the southern Aegean region along the northern African promontory (McClusky *et al*. 2000). Although it is impossible to identify the individual faults that accommodated the two counterclockwise Plio-Pleistocene rotation phases, it is likely that the currently active left-lateral strike-slip system associated with the offshore Pliny and Strabo trenches is responsible for the observed rotations.

The explanation we advocate for the vertical motions of Rhodos involves motion along normal faults and a well-constrained thrust fault. The rotational motion, however, fits best in a context of strike-slip faulting. All such faults have been defined in the southeastern Aegean region. However, our data conclusively show alternating phases of vertical and rotational motions. The implication of our interpretations is that the net motion of Rhodos is partitioned along strike-slip faults and alternates with motion along normal faults or thrust faults, although we note that we cannot confirm this implication by an independent third method.

To date, only the present-day structure of Rhodos and offshore imagery have been used to infer the age of the Pliny and Strabo trenches (ten Veen & Kleinspehn 2002), together with the observation of Woodside *et al*. (2000) that the offshore deep-marine Rhodos basin does not contain any Messinian evaporites and therefore postdates the Miocene. Our new data from Rhodos provide accurate vertical and rotational motions that accompanied the formation of these structures, and allow us to put minimum time constraints on the activity of the Pliny and Strabo trenches: these should at least have been active since 3.8 Ma, and possibly earlier. This is in line with vertical motion information obtained from Crete, which as a result of the wrenching along the Pliny and Strabo trenches was uplifted some time during the early to middle Pliocene (Meulenkamp *et al*. 1994; van Hinsbergen & Meulenkamp 2006).

This observation has important implications for the various geodynamic scenarios that have been suggested for the Aegean region. Cornée *et al*. (2006*b*) loosely correlated the drowning of the southeastern coast of Rhodos to the westward motion of Anatolia. A first correlation presented here correlated the drowning of this part of Rhodos and the younger rotation history of the island to the formation of the Pliny and Strabo strike-slip system, and considers the foundering of the Rhodos basin as the structural termination this system. It seems reasonable to associate the Pliny and Strabo trenches with the westward propagation of Anatolia into the Aegean domain, because the Pliny and Strabo strike-slip faults start their activity within the same time interval (early Pliocene) as the formation of the north Aegean trough and the Marmara pull-apart basin (Armijo *et al*. 1999). The latter two form the expression of the propagation of the right-lateral North Anatolian Fault Zone into the Aegean region. Thus, in the early Pliocene, two strike-slip systems penetrated the Aegean region, a right-lateral one in the north and a left-lateral one in the south, which accommodate the westward motion of the Aegean region together with Anatolia.

As already noted by Armijo *et al*. (2004) and Flerit *et al*. (2004), the westward motion of Anatolia alone cannot explain the deformation field of the Aegean region since the Pliocene. Global positioning system observations and modelling studies show that the Aegean region, including the southeastern segment, underwent a deformation superimposed on the motion induced by Anatolia (McClusky *et al*. 2000; Kreemer & Chamot-Rooke 2004). For Rhodos, this means a component of motion towards the SE, subperpendicular to the thrust fault that is used to explain the uplift and northwestward tilt of Rhodos. An existing scenario to explain this additional component in the Aegean deformation concerns gravitational spreading of the Aegean region towards and over the subducting African plate (Meijer & Wortel 1997; Gautier *et al*. 1999). The predictions from this model are in line with the observations from Rhodos, but we have no means to independently test it. The gravitational spreading can be triggered by roll-back of the subducted plate (Le Pichon & Angelier 1979; Meulenkamp *et al*. 1988). Recently, Govers & Wortel (2005) have explained the formation of the Pliny and Strabo trenches as the surface expression of a subduction-transform edge-propagator (STEP) fault, which would accommodate the change from southward to southwestward roll-back of the African plate. This scenario implies that the Pliny and Strabo strike-slip faults become younger from east to west. Our new data allow the testing of this implication. The first expression on Rhodos of the generation of the strike-slip system is here reconstructed between 5.3 Ma (end of the Miocene) and 3.8 Ma (when the first rotation affects Rhodos). On Crete, the first expression is loosely dated some time during the early Pliocene between 5.3 and 3.5 Ma (van Hinsbergen & Meulenkamp 2006). Therefore, a clear lateral temporal trend in onset of activity of the Pliny and Strabo strike-slip system cannot be confirmed.

Conclusions

In this paper, we reconstruct and accurately date Plio-Pleistocene motions of the island of Rhodos in the southeastern Aegean forearc. A new magnetostratigraphic framework for the Apolakkia basin fill on southwestern Rhodos is presented, and a recently published chronostratigraphy of the late Plio-Pleistocene stratigraphy of northern and eastern Rhodos is incorporated. The resulting time frame, in combination with palaeomagnetic and palaeobathymetric analysis of a large number of sedimentary sections, allows us to subdivide the Plio-Pleistocene tectonic history of Rhodos into four discrete phases following the late Miocene–early Pliocene extension phase that opened the Apo-

lakkia basin. These are as follows: (1) between 3.8 and 3.6 Ma, a $9 \pm 6°$ counterclockwise rotation phase; (2) between 2.5 and 1.8 Ma, Rhodos tilted to the SE, drowning the southeastern coast to a depth of *c*. 500–600 m; (3) between 1.5 and 1.1 Ma, Rhodos tilted to the NW, and the drowned relief re-emerged; (4) since 0.8 Ma, a $17 \pm 5°$ counterclockwise rotation.

It is unlikely that the rotations of Rhodos coincide with the post-early Miocene 30° ccw rotation of the Bey Dağları region in southwestern Turkey, as this would imply an amount of extension to accommodate the rotation in eastern Greece and western Turkey that is orders of magnitude more than observed. More likely, the rotations of Rhodos are related to the incipient formation of the south Aegean sinistral strike-slip system and the foundering of the Rhodos basin. Previously shown absence of Messinian evaporites in the deep-marine Rhodos basin in combination with the 3.8 Ma onset of counterclockwise rotation of Rhodos constrains the onset of the formation of the south Aegean strike-slip system between 5.3 and 3.8 Ma. The formation of this strike-slip system is probably related to the interplay of oblique collision between the southeastern Aegean region and the northward moving African plate, the westward motion of Anatolia, gravitational spreading of the overthickened Aegean lithosphere and the recently postulated southwestward retreat of the African subducted slab along a STEP fault.

The investigations were supported by the Netherlands Council for Earth and Life Sciences (ALW) of the Netherlands Organisation for Scientific Research (NWO). D.J.J.v.H. is supported by an NWO VENI grant. J.-J.C. acknowledges IUF support and thanks P. Moisette, C. Lécuyer, P. Desvignes, F. Quillévéré and S. Joannin for participating in the field-trip. F. Hilgen and E. Turco are thanked for the biostratigraphic age dating. This paper is based on work carried out during several field trips on Rhodos, and we acknowledge the pleasant and fruitful co-operation in the field with D. Duranti, J. Steenbrink, J. Meulenkamp, F. Hilgen, M. Dekkers, S. Ernst and E. Snel. We acknowledge the valuable comments of two anonymous reviewers. This work was conducted under the programme of the Dutch Vening Meinesz Research School of Geodynamics (VMSG). This is UMR contribution 5125-07.017.

References

Agustí, J. 2001. A calibrated mammal scale for the Neogene of western Europe. State of the art. *Earth-Science Reviews*, **52**, 247–260.

Armijo, R., Meyer, B., Hubert, A. & Barka, A. 1999. Westward propagation of the North Anatolian fault into the northern Aegean: timing and kinematics. *Geology*, **27**, 267–270.

Armijo, R., Flerit, F., King, G. & Meyer, B. 2004. Linear elastic fracture mechanics explains the past and present evolution of the Aegean. *Earth and Planetary Science Letters*, **217**, 85–95.

Beck, M.E., Burmester, R.F., Kondopoulou, D.P. & Atzemoglou, A. 2001. The palaeomagnetism of Lesbos, NE Aegean, and the eastern Mediterranean inclination anomaly. *Geophysical Journal International*, **145**, 233–245.

Benda, L., Meulenkamp, J.E. & Van de Weerd, A. 1977. Biostratigraphic correlations in the Eastern Mediterranean Neogene. 3. Correlation between mammal, sporomorph and marine microfossil assemblages from the Upper Cenozoic of Rhodos, Greece. *Newsletters in Stratigraphy*, **6**, 117–130.

Bornovas, I. & Rontogianni-Tsiabaou, T. 1983. *Geological map of Greece, 1:500 000*. Institute of Geology and Mineral Exploration, Athens.

Broekman, J.A. 1974. Sedimentation and paleoecology of Pliocene Lagoonal–shallow marine deposits on the island of Rhodos (Greece). *Utrecht Micropaleontological Bulletins*, **6**, 1–142.

Cornée, J.J., Moissette, P. & Joannin, S. *et al*. 2006a. Tectonic and climatic controls of coastal sedimentation: the Late Pliocene–Middle Pleistocene of northeastern Rhodes. *Sedimentary Geology*, **187**, 159–181.

Cornée, J.J., Münch, P. & Quillévéré, F. *et al*. 2006b. Timing of Late Pliocene to Middle Pleistocene tectonic events in Rhodes (Greece) inferred from magneto-biostratigraphy and $^{40}Ar/^{39}Ar$ dating of a volcaniclastic layer. *Earth and Planetary Science Letters*, **250**, 281–291.

de Bruijn, H., Dawson, M.R. & Mein, P. 1970. Upper Pliocene Rodentia, Lagomorpha and Insectivora (mammalia) from the isle of Rhodos (Greece). *Proceeding, Koninklijke Nederlandse Akademie van Wetenschappen, Series B*, **B73**, 535–584.

Dewey, J.F. & Sengör, A.M.C. 1979. Aegean and surrounding regions: complex multiplate and continuum tectonics in a convergent zone. *Geological Society of America Bulletin*, **90**, 84–92.

Duermeijer, C.E., Krijgsman, W., Langereis, C.G. & ten Veen, J.H. 1998. Post early Messinian counter-clockwise rotations on Crete: implications for the late Miocene to Recent kinematics of the southern Hellenic Arc. *Tectonophysics*, **298**, 77–89.

Duermeijer, C.E., Krijgsman, W., Langereis, C.G., Meulenkamp, J.E., Triantaphyllou, M.V. & Zachariasse, W.J. 1999. A Late Pleistocene clockwise rotation phase of Zakynthos (Greece) and implications for the evolution of the western Aegean arc. *Earth and Planetary Science Letters*, **173**, 315–331.

Duermeijer, C.E., Nyst, M., Meijer, P.T., Langereis, C.G. & Spakman, W. 2000. Neogene evolution of the Aegean arc: paleomagnetic and geodetic evidence for a rapid and young rotation phase. *Earth and Planetary Science Letters*, **176**, 509–525.

Duranti, D. 1997. *Il 'Levantino' fluvio-lacustre dell isola di Rodi (Grecia). Sedimentologia ed analisi di bacino*. PhD Thesis, University of Bologna.

Fisher, R.A. 1953. Dispersion on a sphere. *Proceedings of the Royal Society of London, Series A*, **217**, 295–305.

Flerit, F., Armijo, R., King, G. & Meyer, B. 2004. The mechanical interaction between the propagating North Anatolian Fault and the back-arc extension in the Aegean. *Earth and Planetary Science Letters*, **224**, 347–362.

Frydas, D. 1994. Die Pliozän/Pleistozän-Grenze auf der Insel Rhodos (Griechenland). *Münstersche Forschungen zur Geologie und Paläontologie*, **76**, 331–344.

Gautier, P., Brun, J.-P., Moriceau, R., Sokoutis, D., Martinod, J. & Jolivet, L. 1999. Timing, kinematics and cause of Aegean extension: a scenario based on a comparison with simple analogue experiments. *Tectonophysics*, **315**, 31–72.

Govers, R. & Wortel, M.J.R. 2005. Lithosphere tearing at STEP faults: response to edges of subduction zones. *Earth and Planetary Science Letters*, **236**, 505–523.

Hanken, N.-M., Bromley, R. & Miller, J. 1996. Plio-Pleistocene sedimentation in coastal grabens, North-east Rhodes, Greece. *Geological Journal*, **31**, 271–296.

Hansen, K.S. 1999. Development of a prograding carbonate wedge during sea level fall: Lower Pleistocene of Rhodos, Greece. *Sedimentology*, **46**, 559–576.

Huguen, C., Mascle, J., Chaumillon, E., Woodside, J.M., Benkhelil, A. & Volkonskaïa, A. 2001. Deformational styles of the eastern Mediterranean Ridge and surroundings from combined swath mapping and seismic reflection profiling. *Tectonophysics*, **343**, 21–47.

Jolivet, L. 2001. A comparison of geodetic and finite strain pattern in the Aegean, geodynamic implications. *Earth and Planetary Science Letters*, **187**, 95–104.

Kirschvink, J.L. 1980. The least-squares line and plane and the analysis of palaeomagnetic data. *Geophysical Journal of the Royal Astronomical Society*, **62**, 699–718.

Kissel, C. & Poisson, A. 1987. Étude paléomagnetique préliminaire des formations cénozoïques des Bey Daglari (Taurides occidentales, Turquie). *Comptes Rendus de l'Académie des Sciences, Série II*, **304**, 343–348.

Kissel, C., Laj, C., Sengör, A.M.C. & Poisson, A. 1987. Paleomagnetic evidence for rotation in opposite senses of adjacent blocks in northeastern Aegean and western Anatolia. *Geophysical Research Letters*, 14, 907–910.

Kissel, C., Laj, C., Poisson, A. & Simeakis, K. 1989. A pattern of block rotations in central Aegea. *In:* Kissel, C. & Laj, C. (eds) *Paleomagnetic Rotations and Continental Deformation*. Kluwer, Dordrecht, 115–129.

Kondopoulou, D., De Bonis, L., Koufos, G. & Sen, S. 1993. Paleomagnetic data and biostratigraphy of the Middle Miocene vertebrate locality of Thymiana, Chios island, Greece. *In: Proceedings of the 2nd Congress of the Hellenic Geophysical Union, Florina*. 676–687.

Kondopoulou, D.P. 1982. *Paleomagnétisme et déformations néogènes du Nord de la mer Egée*. PhD Thesis, Université de Strasbourg.

Kontogianni, V.A., Tsoulos, N. & Stiros, S.C. 2002. Coastal uplift, earthquakes and active faulting of Rhodes Island (Aegean Arc): modeling based on geodetic inversion. *Marine Geology*, **186**, 299–317.

Kovacs, E. & Spjeldnæs, N. 1999. Pliocene–Pleistocene stratigraphy of Rhodes, Greece. *Newsletters in Stratigraphy*, **37**, 191–208.

Kreemer, C. & Chamot-Rooke, N. 2004. Contemporary kinematics of the southern Aegean and the Mediterranean Ridge. *Geophysical Journal International*, **157**, 1377–1392.

Krijgsman, W. & Tauxe, L. 2004. Shallow bias in the Mediterranean paleomagnetic directions caused by inclination error. *Earth and Planetary Science Letters*, **222**, 685–695.

Krijgsman, W., Leewis, M.E., Garces, M., Kouwenhoven, T.J., Kuiper, K.F. & Sierro, F.J. 2006. Tectonic control for evaporite formation in the Eastern Betics (Tortonian; Spain). *Sedimentary Geology*, **188-189**, 155–170.

Laj, C., Gauthier, A.J. & Keraudren, B. 1978. Mise en évidence d'úne rotation plio-quarternaire de l'île de Rhodes (Grèce): résultats préliminaires. *Réunion Annulaire de Sciences de la Terre*, **6e Orsay**, 224.

Laj, C., Jamet, M., Sorel, D. & Valente, J.P. 1982. First paleomagnetic results from Mio-Pliocene series of the Hellenic sedimentary arc. *Tectonophysics*, **86**, 45–67.

Le Pichon, X. 1982. Land-locked oceanic basins and continental collision: the Eastern Mediterranean as a case example. *In:* Hsü, K.J. (ed.) *Mountain Building Processes*. Academic Press, London, 201–211.

Le Pichon, X. & Angelier, J. 1979. The Hellenic arc and trench system: a key to the neotectonic evolution of the Eastern Mediterranean area. *Tectonophysics*, **60**, 1–42.

Lourens, L.J., Hilgen, F.J. & Raffi, I. 1998. Base of large *Gephyrocapsa* and astronomical calibration of early Pleistocene sapropels in site 967 and Hole 969D: solving the chronology of the Vrica section (Calabria, Italy). *In:* Robertson, A.H.F., Emeis, K.C., Richter, C. & Camerlenghi, A. (eds) *Proceedings of the Ocean Drilling Program, Scientific Results, 160*. Ocean Drilling Program, College Station, TX, 191–197.

Lourens, L.J., Hilgen, F.J., Laskar, J., Shackleton, N.J. & Wilson, D. 2004. The Neogene Period. *In:* Gradstein, F.M., Ogg, J.G. & Smith, A.G. (eds) *A Geologic Time Scale 2004*. Cambridge University Press, Cambridge, 409–440.

Løvlie, R. & Hanken, N.-M. 2002. Conglomerate test of non-lithified Plio-Pleistocene marine sediments and rock magnetic constrains suggests pDRM type remagnetisation. *Physics and Chemistry of the Earth*, **27**, 1121–1130.

Løvlie, R., Støle, G. & Spjeldnæs, N. 1989. Magnetic polarity stratigraphy of Pliocene–Pleistocene marine sediments from Rhodos, eastern Mediterranean. *Physics of the Earth and Planetary Interiors*, **54**, 340–352.

Mascle, J., Le Cleac'h, A. & Jongsma, D. 1986. The eastern Hellenic margin from Crete to Rhodes: example of progressive collision. *Marine Geology*, **73**, 145–168.

Mascle, J., Huguen, C. & Benkhelil, J. *et al.* 1999. Images may show start of European–African plate collision. *EOS Transactions, American Geophysical Union*, **80**, 421–428.

McClusky, S., Balassanian, S. & Barka, A. *et al.* 2000. Global Positioning System constraints on plate kinematics and dynamics in the eastern Mediterranean and Caucasus. *Journal of Geophysical Research*, **105**, 5695–5719.

McFadden, P.C. & McElhinny, M.W. 1990. Classification of the reversal test in palaeomagnetism. *Geophysical Journal International*, **103**, 725–729.

McFadden, P.L. 1990. A new fold-test for palaeomagnetic studies. *Geophysical Journal International*, **103**, 163–169.

McFadden, P.L. & Jones, F.J. 1981. The discrimination of mean directions drawn from Fisher distributions. *Geophysical Journal of the Royal Astronomical Society*, **67**, 19–33.

Meijer, P.T. & Wortel, M.J.R. 1997. Present-day dynamics of the Aegean region: a model analysis of the horizontal pattern of stress and deformation. *Tectonics*, **16**, 879–895.

Meulenkamp, J.E., De Mulder, E.F.J. & Van de Weerd, A. 1972. Sedimentary history and paleogeography of the Late Cenozoic of the island of Rhodos. *Zeitschrift der Deutschen Geologischen Gesellschaft*, **123**, 541–553.

Meulenkamp, J.E., Wortel, M.J.R., Van Wamel, W.A., Spakman, W. & Hoogerduyn Strating, E. 1988. On the Hellenic subduction zone and the geodynamical evolution of Crete since the late Middle Miocene. *Tectonophysics*, **146**, 203–215.

Meulenkamp, J.E., Van der Zwaan, G.J. & Van Wamel, W.A. 1994. On Late Miocene to Recent vertical motions in the Cretan segment of the Hellenic arc. *Tectonophysics*, **234**, 53–72.

Moissette, P. & Spjeldnæs, N. 1995. Plio-Pleistocene deep-water bryozoans from Rhodes, Greece. *Paleontology*, **38**, 771–799.

Morris, A. & Robertson, A.H.F. 1993. Miocene remagnetisation of carbonate platform and Antalya Complex units within the Isparta Angle, SW Turkey. *Tectonophysics*, **220**, 243–266.

Mutti, E., Orombelli, G. & Pozzi, R. 1970. Geological studies on the Dodecanese islands (Aegean Sea). IX. Geological map of the island of Rhodes (Greece). Explanatory notes. *Annuaire Géologique de Pays Hellénique*, **22**, 77–226.

Peters, J.M. & Huson, W.J. 1985. The Pliny and Strabo trenches (Eastern Mediterranean): integration of seismic reflection data and SeaBeam bathymetry maps. *Marine Geology*, **64**, 1–17.

Sen, S. & Valet, J.-P. 1986. Magnetostratigraphy of late Miocene continental deposits in Samos, Greece. *Earth and Planetary Science Letters*, **80**, 167–174.

Sørensen, M. 1984. Growth and mortality in two Pleistocene bathyal micromorphic bivalves. *Lethaia*, **17**, 197–210.

Spaak, P. 1983. *Accuracy in correlation and ecological aspects of the planktonic foraminiferal zonation of the Mediterranean Pliocene*. Utrecht Micropaleontological Bulletins, **28**.

Tauxe, L. & Kent, D.V. 2004. A simplified statistical model for the geomagnetic field and the detection of shallow bias in paleomagnetic inclinations: was the ancient magnetic field dipolar? *In:* Channell, J.E.T. *et al.* (ed.) *Timescales of the Paleomagnetic Field*. Geophysical Monograph, American Geophysical Union, **145**, 101–116.

Taymaz, T., Jackson, J. & McKenzie, D. 1991. Active tectonics of the north and central Aegean Sea. *Geophysical Journal International*, **106**, 433–490.

ten Veen, J.H. & Kleinspehn, K.L. 2002. Geodynamics along an increasingly curved convergent plate margin; late Miocene–Pleistocene Rhodes, Greece. *Tectonics*, **21**, 21.

ten Veen, J.H. & Kleinspehn, K.L. 2003. Incipient continental collision and plate-boundary curvature: Late Pliocene–Holocene transtensional Hellenic forearc, Crete, Greece. *Journal of the Geological Society, London*, **160**, 161–181.

ten Veen, J.H. & Meijer, P.T. 1998. Late Miocene to Recent tectonic evolution of Crete (Greece): geological observations and model analysis. *Tectonophysics*, **298**, 191–208.

ten Veen, J.H. & Postma, G. 1999. Neogene tectonics and basin fill patterns in the Hellenic outer-arc (Crete, Greece). *Basin Research*, **11**, 243–266.

Thomsen, E., Rasmussen, T.L. & Hastrup, A. 2001. Calcareous nannofossil, ostracode and foraminifera biostratigraphy of Plio-Pleistocene deposits, Rhodes (Greece, with a correlation to the Vrica section (Italy). *Journal of Micropaleontology*, **20**, 143–154.

Titschack, J., Bromley, R.G. & Freiwald, A. 2005. Plio-Pleistocene cliff-bound, wedge-shaped, warm-temperate carbonate deposits from Rhodes (Greece): sedimentology and facies. *Sedimentary Geology*, **180**, 29–56.

van der Meulen, M.J., Kouwenhoven, T.J., Van der Zwaan, G.J., Meulenkamp, J.E. & Wortel, M.J.R. 1999. Late Miocene uplift in the Romagnian Apennines and the detachment of subducted lithosphere. *Tectonophysics*, **315**, 319–335.

van der Meulen, M.J., Buiter, S.J.H., Meulenkamp, J.E. & Wortel, M.J.R. 2000. An Early Pliocene uplift of the central Apenninic foredeep, and its geodynamic significance. *Tectonics*, **19**, 300–313.

van der Zwaan, G.J., Jorissen, F.J. & De Stigter, H.C. 1990. The depth dependency of planktonic/benthonic foraminiferal ratios: constraints and applications. *Marine Geology*, **95**, 1–16.

van de Weerd, A.J., Reumer, W.F. & De Vos, J. 1982. Pliocene mammals from the Apolakia Formation (Rhodes, Greece). *Proceeding, Koninklijke Nederlandse Akademie van Wetenschappen, Series B*, **85**, 89–112.

van Hinsbergen, D.J.J. & Meulenkamp, J.E. 2006. Neogene supra-detachment basin development on Crete (Greece) during exhumation of the South Aegean core complex. *Basin Research*, **18**, 103–124.

van Hinsbergen, D.J.J., Snel, E., Garstman, S.A., Marunteanu, M., Langereis, C.G., Wortel, M.J.R. & Meulenkamp, J.E. 2004. Vertical motions in the Aegean volcanic arc: evidence for rapid subsidence preceding *in situ* volcanism. *Marine Geology*, **209**, 329–345.

van Hinsbergen, D.J.J., Kouwenhoven, T.J. & van der Zwaan, G.J. 2005a. Paleobathymetry in the backstripping procedure: correction for oxygenation effects on depth estimates. *Palaeogeography, Palaeoclimatology, Palaeoecology*, **221**, 245–265.

van Hinsbergen, D.J.J., Langereis, C.G. & Meulenkamp, J.E. 2005b. Revision of the timing, magnitude and distribution of Neogene rotations in the western Aegean region. *Tectonophysics*, **396**, 1–34.

van Hinsbergen, D.J.J., van der Meer, D.G., Zachariasse, W.J. & Meulenkamp, J.E. 2006. Deformation of western Greece during Neogene clockwise rotation and collision with Apulia. *International Journal of Earth Sciences*, **95**, 463–490.

van Vugt, N. 2000. Orbital forcing in late Neogene lacustrine basins from the Mediterranean. *Geologica Ultraiectina*, **189**, 1–167.

Willmann, R. 1980. Die Alterstellung kontinentales Neogen-ablagerungen in der Subostlichen Agais (Rhodos und Kos/Dodekanesos, Datca/Subwestanatolien). *Newsletters in Stratigraphy*, **9**, 1–18.

Woodside, J., Mascle, J., Huguen, C. & Volkonskaia, A. 2000. The Rhodes basin, a post-Miocene tectonic trough. *Marine Geology*, **165**, 1–12.

Received 3 May 2006; revised typescript accepted 7 March 2007.
Scientific editing by Ellen Platzman